Crucial role of a shared extracellular loop in apamin sensitivity and maintenance of pore shape of small-conductance calcium-activated potassium (SK) channels

Kate L. Weatherall[a], Vincent Seutin[b], Jean-François Liégeois[c], and Neil V. Marrion[a,1]

[a]School of Physiology and Pharmacology, University of Bristol, Bristol BS8 1TD, United Kingdom; and Laboratories of [b]Pharmacology and Groupe Interdisciplinaire de Génoprotéomique Appliquée-Neuroscience and [c]Centre Interfacultaire de Recherche du Médicament, University of Liège, B-4000 Liège, Belgium

Edited by Michael D. Cahalan, University of California, Irvine, CA, and approved September 29, 2011 (received for review July 3, 2011)

Activation of small-conductance calcium (Ca^{2+})-dependent potassium ($K_{Ca}2$) channels (herein called "SK") produces membrane hyperpolarization to regulate membrane excitability. Three subtypes (SK1–3) have been cloned and are distributed throughout the nervous system, smooth muscle, and heart. It is difficult to discern the physiological role of individual channel subtypes as most blockers or enhancers do not discriminate between subtypes. The archetypical blocker apamin displays some selectivity between SK channel subtypes, with SK2 being the most sensitive, followed by SK3 and then SK1. Sensitivity of SK1 is species specific, with the human isoform being blocked by the toxin, whereas the rat is not. Mutation studies have identified residues within the outer pore that suggest apamin blocks by an allosteric mechanism. Apamin also uses a residue within the S3–S4 extracellular loop to produce a high-sensitivity block. We have identified that a 3-amino acid motif within this loop regulates the shape of the channel pore. This motif is required for binding and block by apamin, suggesting that a change in pore shape underlies allosteric block. This motif is absent in rat SK1, explaining why it is insensitive to block by apamin. The overlapping distribution of SK channel subtype expression suggests that native heteromeric channels may be common. We show that the S3–S4 loop of one subunit overlaps the outer pore of the adjacent subunit, with apamin interacting with both regions. This arrangement provides a unique binding site for each combination of SK subunits within a coassembled channel that may be targeted to produce blockers specific for heteromeric SK channels.

patch clamp | afterhyperpolarization

Pharmacological modulation of small-conductance Ca^{2+}-activated potassium (SK/$K_{Ca}2$) channels has been suggested as a potential target for a number of disorders including dementia, depression, and cardiac arrhythmias. Three subtypes of SK channel have been cloned, with distinct but partially overlapping expression patterns (1–3). A nonpeptidic subtype-specific blocker of SK channels has yet to be developed. The lack of SK subtype selective blockers combined with this wide distribution means that their roles cannot be well defined. This lack of specificity also means that current available SK blockers have a very narrow therapeutic window, with an overlap of doses required for therapeutic benefit and those producing toxic effects in animal studies (4).

SK channels are blocked by the bee venom toxin apamin, which displays weak subtype selectivity. The toxin is most potent at SK2 (IC_{50} ~ 70 pM) (5–9) and SK3 (IC_{50} ~ 0.63–6 nM) (7, 9, 10), followed by the human isoform of SK1 (IC_{50} ~ 1–8 nM) (8, 9), whereas the rat isoform of SK1 is apamin insensitive (11, 12). Mutation studies have identified a number of residues within the outer pore that affect block by apamin (7, 8, 13). For example, an outer pore histidine residue has been shown to be critical for both binding and block by the toxin (7). Structural modeling has placed apamin binding with the channel outer pore, interacting with this critical histidine residue (7). These data suggested that apamin does not behave as a classical pore blocker, but blocks using an allosteric mechanism (7). Apamin also interacts with a serine residue in the S3–S4 extracellular loop to impart a high-sensitivity block of SK2, with mutation of the corresponding threonine in hSK1 to a serine increasing sensitivity of block of hSK1 by the toxin (8). Block of SK channel current by apamin is clearly more complicated than these data suggest, as despite containing an identical outer pore sequence to the apamin-sensitive hSK1 and a serine in this position in the S3–S4 loop, rSK1 is apamin insensitive. Replacement of the S3–S4 loop of rSK1 with that of hSK1 produced a channel with a sensitivity to apamin that was similar to that of hSK1 (8). These data indicate that an additional interaction site(s) within the S3–S4 extracellular loop contributes to binding or block by apamin. We have used a combination of mutagenesis, functional block, and radioligand binding to determine that two amino acids in the S3–S4 loop affect the shape of the outer and inner pore region of the channel and are critical for apamin binding and block. Crucially, these findings reveal that due to differences in the S3–S4 loop sequence, the rat and human isoforms of SK1 have unique pore structures that result in a significant difference in their sensitivity both to apamin and to a number of SK channel pore blockers. Overlapping distributions of SK channel subunits suggest that formation of heteromeric channels occurs in vivo (2). Coexpression of apamin-insensitive rSK1 subunits or a loop mutant of rSK2, with apamin-sensitive rSK2 subunits, produces apamin-sensitive current. The difference in sensitivity to block of these heteromeric channel currents by apamin suggests that the binding site for the toxin is formed by two adjacent subunits, the outer pore region of one and the S3–S4 loop of the adjacent subunit. This proposal is confirmed by producing apamin-sensitive current from coexpression of two apamin-insensitive rSK2 mutant subunits, one with a disrupted S3–S4 loop region and one with a disrupted outer pore region. We show that the interface between these two regions provides a unique target that will depend on the SK subtypes contributing to the heteromer.

Results

Role of the S3–S4 Extracellular Loop in Binding and Block of SK Channels by Apamin. ***Role of single amino acid residues in the binding and block by apamin of SK channel currents.*** Alignment of the amino acid sequence of the S3–S4 extracellular loop of various SK channel subtypes shows a three-amino-acid motif that differs between subtypes (Fig. 1). Mutation of serine 245 in rSK2 to mimic the three-amino-acid motif found in hSK1 [rSK2(S245T)]

Author contributions: K.L.W. and N.V.M. designed research; K.L.W., V.S., and J.-F.L. performed research; K.L.W. and J.-F.L. analyzed data; and K.L.W. and N.V.M. wrote the paper.

The authors declare no conflict of interest.

This article is a PNAS Direct Submission.

[1]To whom correspondence should be addressed. E-mail: N.V.Marrion@bris.ac.uk.

This article contains supporting information online at www.pnas.org/lookup/suppl/doi:10.1073/pnas.1110724108/-/DCSupplemental.

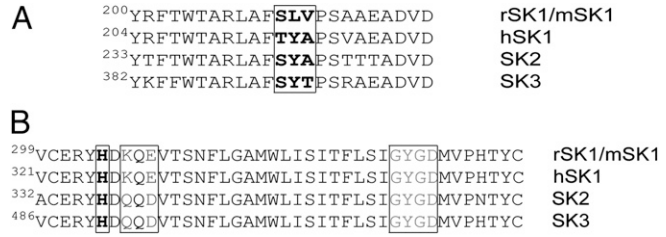

Fig. 1. Alignment of the (*A*) S3–S4 extracellular loop and (*B*) pore region sequences of SK channel subtypes. Shown is sequence alignment of the S3–S4 loop (*A*) and pore region (*B*) of rSK1/mSK1, hSK1, SK2, and SK3. S3–S4 loop regions of rat, human, and mouse isoforms of SK2 and SK3 are identical, as are the pore sequences of human and rat SK1. Amino acid residues within the S3–S4 loop that are mutated are boxed and shown in boldface type. The histidine residue critical for both binding and block by apamin within the outer pore region is boxed and shown in boldface type. The lysine/glutamine and glutamate/aspartate residues of the outer pore known to affect apamin sensitivity are boxed and shown in dark gray. The signature selectivity sequence with the pore region for K^+ channels is boxed and shown in light gray.

produces an inward rectifying current that exhibits a lower sensitivity to block by apamin than wild-type rSK2 (rSK2 IC_{50}, 69.5 ± 13.3 pM, $n = 6$; rSK2(S245T) IC_{50}, 529 ± 59 pM, $n = 6$, $P < 0.0001$) (Fig. 2 *A* and *C* and Table 1). This shift in apamin sensitivity (~eightfold) is less than that reported for the opposite mutation (~19-fold) (10). The lower sensitivity observed here directly results from a reduction in binding affinity for the toxin, with the affinity of binding (K_D) to rSK2 being 5.3 ± 1.5 pM ($n = 4$), whereas ^{125}I-apamin binding to rSK2(S245T) exhibits a K_D of 31.3 ± 5.4 pM ($n = 3$) (Table 1). The corresponding residue in rSK1 cannot explain its apamin insensitivity (Fig. 3*A*), as this subunit possesses a serine residue in this position (Fig. 1). Sequence alignment of the S3–S4 loop regions of rSK1 and SK2 shows a difference of two amino acids (^{246}YA^{247}/^{213}LV^{214}), which may affect the ability of apamin to interact with the channel to cause block. Mutation of tyrosine 246 to the corresponding leucine in rSK1 [rSK2(Y246L)] produces an ~4.5-fold reduction in apamin sensitivity (rSK2 IC_{50}, 69.5 ± 13.3 pM; rSK2 (Y246L) IC_{50}, 311 ± 74 pM, $n = 6$, $P < 0.009$) (Fig. 2 *B* and *C* and Table 1). This reduced sensitivity is mirrored by a similar fold reduction in binding affinity of ^{125}I-apamin (K_D, 20.4 ± 4.4 pM, $n = 3$) (Table 1). Therefore, changes in binding affinity have corresponding effects on the sensitivity to block by apamin of functional current. In contrast, the sensitivity to block by apamin is unaffected by mutation of alanine 247 in the S3–S4 loop to the corresponding valine in rSK1 [rSK2(A247V)] (IC_{50}, 55.5 ± 8.4 pM, $n = 6$, $P = 0.5432$) (Fig. 2*C*). Interestingly, the single point mutations that affect sensitivity to apamin also influence the positive cooperativity of block. The Hill coefficient of wild-type rSK2 is ~2, whereas a Hill coefficient close to unity is observed for the single point mutants (Table 1).

Tetraethylammonium (TEA) and d-tubocurarine (dTC) are used as molecular calipers to detect differences in the inner and outer pore structures of SK channels, respectively (7, 8, 13, 14). TEA blocks by binding to the inner pore (extracellular to the selectivity filter), whereas dTC blocks SK channel currents by interacting with the channel outer pore (7, 13). Wild-type rSK2 is blocked by dTC with an IC_{50} of 4.25 ± 0.52 μM ($n = 6$) (Fig. 2*D*) and TEA with an IC_{50} of 2.18 ± 0.38 mM ($n = 6$) (Fig. 2*E*) (Table 1). Despite causing a significant decrease in the sensitivity to apamin, the single point mutations rSK2(S245T) and rSK2 (Y246L) have no effect on the sensitivity to either dTC (IC_{50}, 4.16 ± 0.65 μM, $n = 6$, $P = 0.8968$; and IC_{50}, 5.49 ± 1.30 μM, $n = 6$, $P = 0.3159$, respectively) (Fig. 2*D*) or TEA (IC_{50}, 1.28 ± 0.19 mM, $n = 6$, $P = 0.3487$; and IC_{50}, 2.34 ± 0.38 mM, $n = 6$, $P = 0.9362$, respectively) (Fig. 2*E*) (Table 1). This result reveals that reductions in apamin sensitivity resulting from point mutations within the S3–S4 loop are not the result of a change in pore

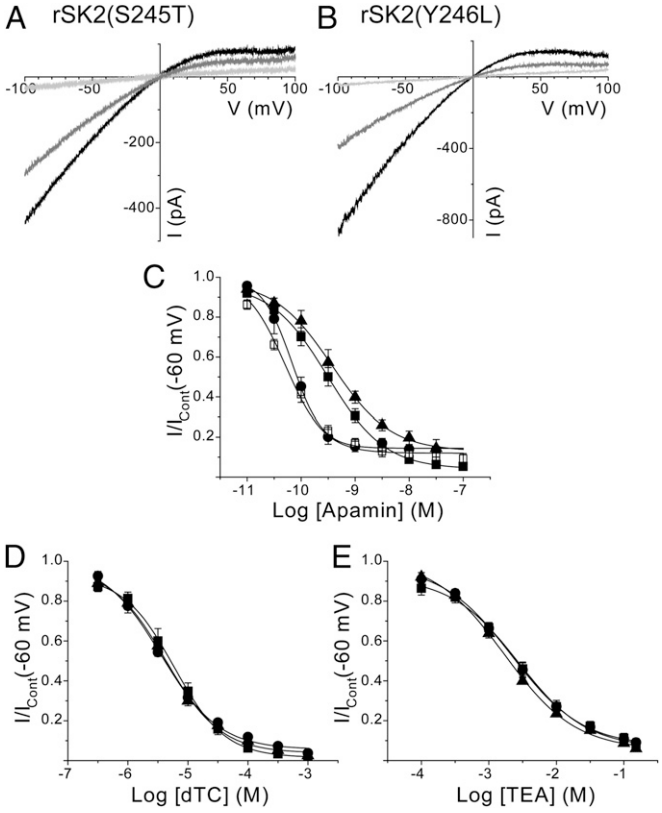

Fig. 2. Effect of single mutations within the S3–S4 loop of rSK2 on the pharmacology of block. (*A*) Outside-out macropatch currents evoked by voltage ramps from −100 to +100 mV of expressed rSK2(S245T) channel subunits in the absence (black) and presence of 300 pM (gray) and 100 nM (light gray) apamin. (*B*) Ramp currents from expressed rSK2(Y246L) channel subunits in the absence (black) and presence of 300 pM (gray) and 100 nM (light gray) apamin. (*C*) Concentration-inhibition relationships for apamin inhibition of expressed rSK2 (●), rSK2(S245T) (▲), rSK2(Y246L) (■), and rSK2 (A247V) (□). (*D* and *E*) Inhibition curves for block by dTC (*D*) and TEA (*E*) for rSK2 (●), rSK2(S245T) (▲), and rSK2(Y246L) (■).

shape, but that apamin appears to interact with the S3–S4 loop directly. These data reveal an amino acid residue, in addition to the serine reported previously (8), that contributes to a high-sensitivity block by apamin. However, these data do not explain why rSK1 is insensitive to block by apamin and it seems possible that this insensitivity might result from the two amino acids in the S3–S4 extracellular loop together that differ from rSK2.

Amino acids ^{246}YA^{247}/^{213}LV^{214} dictate apamin binding and block. Expression of homomeric rSK1 subunits does not produce functional channels (11, 12, 15). Functional channel current is produced on expression of a chimeric channel (rSK1*), where the carboxyl terminus of rSK1 is replaced by that from rSK2 (11). Current resulting from expression of rSK1* is insensitive to apamin (100 nM, $n = 7$, $P = 3436$) (Fig. 3*A*). Two amino acids within the S3–S4 loop motif differ between rSK2 and rSK1, with the ^{246}YA^{247} in rSK2 seen as ^{213}LV^{214} in rSK1 (Fig. 1). Mutation of these two residues in rSK2 to mimic the S3–S4 loop of rSK1 [rSK2(YA246/7LV)] produces a channel current that, like rSK1*, is insensitive to apamin (100 nM, $n = 10$, $P = 0.2932$) (Fig. 3*B*). Insensitivity to apamin results from the toxin not binding to the mutant channel ($n = 4$) (Table 1). These findings suggest that the S3–S4 loop region is required directly for binding of apamin, rather than being required for the allosteric mechanism of block. The reverse mutation, introducing residues into the S3–S4 loop of rSK1* to mimic the S3–S4 loop of rSK2 [rSK1*(LV213/4YA)], results in an apamin-sensitive channel, with an IC_{50} similar to that of hSK1 [rSK1*(LV213/4YA) IC_{50},

Table 1. Comparison of binding and block sensitivities of current produced by expression of wild-type and mutant SK channel subunits

	Apamin		^{125}I-apamin:	dTC		TEA		UCL1684	
	IC_{50} (nM)	n_h	K_D (pM)	IC_{50} (μM)	n_h	IC_{50} (mM)	n_h	IC_{50} (pM)	n_h
rSK2	0.070 ± 0.013	1.9 ± 0.3	5.3 ± 1.5	4.25 ± 0.52	0.8 ± 0.1	2.18 ± 0.38	0.8 ± 0.02	376 ± 100	1.1 ± 0.1
rSK2(S245T)	0.529 ± 0.059	0.9 ± 0.1	31.3 ± 5.4	4.16 ± 0.65	0.9 ± 0.1	1.28 ± 0.19	0.9 ± 0.04	376 ± 101	1.1 ± 0.1
rSK2(Y246L)	0.311 ± 0.074	0.8 ± 0.03	20.4 ± 4.4	5.49 ± 1.30	0.9 ± 0.1	2.34 ± 0.38	0.7 ± 0.1	560 ± 84	0.9 ± 0.1
rSK2(A247V)	0.056 ± 0.008	1.1 ± 0.1							
rSK2(YA246/7LV)	Insensitive		No binding	268 ± 19	0.7 ± 0.1	5.69 ± 0.46	0.8 ± 0.1	Insensitive	
hSK1	1.58 ± 0.26	1.0 ± 0.1		33.3 ± 6.6	0.8 ± 0.1	4.30 ± 0.31	1.0 ± 0.04		
rSK1*	Insensitive			254 ± 30	0.7 ± 0.04	7.51 ± 0.65	1.1 ± 0.2	Insensitive	
rSK1*(LV213/4YA)	1.41 ± 0.43	1.2 ± 0.1		41.5 ± 12.4	0.8 ± 0.1	3.63 ± 0.77	1.0 ± 0.1		

Values are means ± SEM, with appropriate *n* values quoted in the text.

1.41 ± 0.43 nM, $n = 6$; hSK1 IC_{50}, 1.58 ± 0.26 nM, $n = 6$, $P = 0.7688$; Fig. 3*C* and Table 1]. As rSK1 and hSK1 have identical outer pore sequences (Fig. 1), this result suggests that the SLV motif is the sole determinant for the difference in the sensitivity of rSK1 and hSK1 to apamin.

Comparison of the sensitivity to block by dTC showed that differences in the outer pore shape are apparent between wild-type SK channels (rSK2 IC_{50}, 4.25 ± 0.52 μM; rSK1* IC_{50}, 254 ± 30 μM, $n = 6$; hSK1 IC_{50}, 33.3 ± 6.6 μM, $n = 6$, $P < 0.0001$) (Figs. 2*D* and 3*D*) (Table 1). Clearly, the relative insensitivity of rSK1* to block suggests that its pore shape is very different from that of its peers. A similar difference in sensitivity to block by external TEA of rSK1* is apparent, suggesting that the inner pore is of a different shape compared with those of other SK channels (rSK2 IC_{50}, 2.18 ± 0.38 mM, $n = 6$; rSK1* IC_{50}, 7.51 ± 0.65 mM, $n = 6$; hSK1 IC_{50}, 4.30 ± 0.31 mM, $n = 6$. $P < 0.0001$) (Figs. 2*E* and 3*E*) (Table 1). Evaluation of the pore shape of the apamin-insensitive double-loop mutant of SK2 [rSK2(YA246/7LV)] (dTC IC_{50}, 268 ± 19 μM, $n = 6$, $P = 0.7141$, Fig. 3*D* and TEA IC_{50}, 5.69 ± 0.46 mM, $n = 6$, $P < 0.0001$, Fig. 3*E*) (Table 1) shows that it is the same as rSK1*. It is clear that the amino acids ^{246}YA^{247}/^{213}LV^{214} are responsible for the difference in outer pore shape between the two wild-type channels. Mutation of rSK1* to mimic the S3–S4 loop of rSK2 [rSK1(LV213/4YA)] resulted in a shift in sensitivity to dTC and TEA, which was not significantly different from that of hSK1 (dTC IC_{50}, 41.5 ± 12.4 μM, $n = 5$, $P = 0.5513$, Fig. 3*D* and TEA IC_{50}, 3.63 ± 0.77 mM, $n = 7$, $P = 0.4643$, Fig. 3*E*) (Table 1). These findings suggest that the S3–S4 extracellular loop of rSK2 directly interacts with the outer pore region via residues ^{246}YA^{247} to regulate the shape of the pore.

UCL1684 Does Not Use the S3–S4 Extracellular Loop to Block SK Channels. UCL1684 is a potent SK channel current blocker, whose structure includes two quinolinium rings to mimic the arginine residues present within apamin (9, 16). It displaces ^{125}I-apamin binding and has been considered to block using the same mechanism as the toxin (17). Consistent with this proposal, expressed rSK2 channel current is blocked by UCL1684 (IC_{50}, 376 ± 100 pM, $n = 6$) (Fig. 4*A* and Table 1) whereas rSK1* current is insensitive (100 nM, $P = 6$, $P = 0.9495$) (Fig. 4*B*). The apamin-insensitive double-loop mutant of rSK2 [rSK2(YA246/7LV)] is also insensitive to UCL1684 ($n = 6$) (Fig. 4*C*). These data support the proposal that UCL1684 blocks SK channel current using the same mechanism as apamin. However, both rSK1* and the rSK2 mutant rSK2(YA246/7LV) possess very different pore shapes compared with wild-type rSK2 and it is

Table 2. Comparison of block sensitivities of current produced by coexpression of wild-type and mutant SK channel subunits

	Apamin			
	IC_{50} (nM)		n_h	
	a	b	a	b
rSK2-rSK1*	0.450 ± 0.095	8.41 ± 3.38	1.9 ± 0.2	1.1 ± 0.3
rSK2-rSK2(YA246/7LV)	0.117 ± 0.014	19.9 ± 2.51	2.8 ± 0.2	1.2 ± 0.1

Values are means ± SEM, with appropriate *n* values quoted in the text. Headings "a" and "b" correspond to the high- and low-sensitivity components of block observed for current produced by coexpression of different subunits (see text for details).

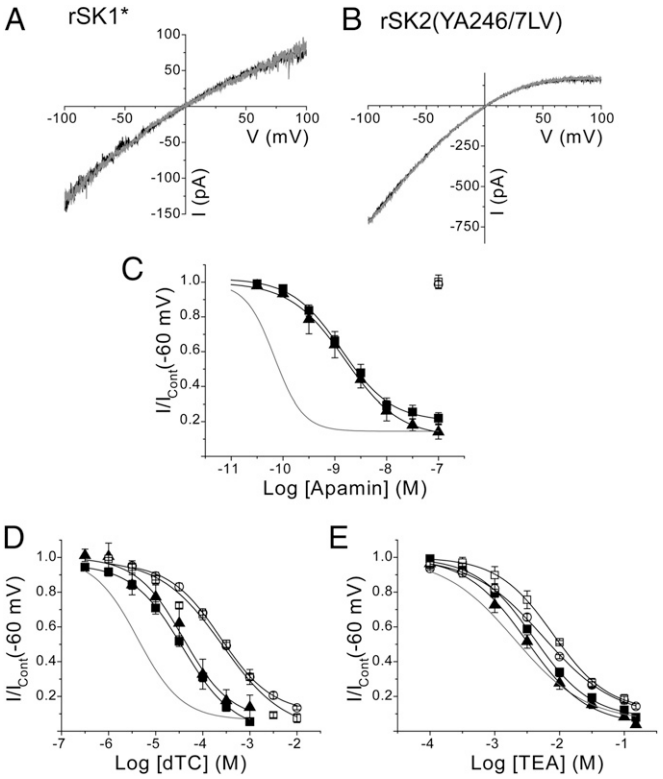

Fig. 3. A two-amino-acid motif in the S3–S4 extracellular loop of SK channels determines apamin sensitivity and pore shape. (*A*) rSK1*-mediated currents evoked by a voltage ramp from −100 to +100 mV in the absence (black) and presence (gray) of apamin (100 nM), showing that rSK1* is insensitive to the toxin. (*B*) Apamin-insensitive current is also produced by expression of rSK2(YA246/7LV) subunits. (*C*) Concentration-inhibition relationships for apamin inhibition of expressed rSK1* (□), rSK2(YA246/7LV) (○), rSK1(LV213/4YA) (▲), and hSK1 (■). (*D* and *E*) Inhibition curves for block by dTC (*D*) and TEA (*E*) for rSK1* (□), rSK2(YA246/7LV (○),rSK1(LV213/4YA) (▲) and hSK1 (■). Inhibition curves for block of rSK2 are shown in gray for comparison.

possible that this difference would prevent block by UCL1684. Point mutations in the S3–S4 extracellular loop that affect apamin block [rSK2(S245T) and rSK2(Y246L)] (Fig. 2 *A* and *B*) had no effect on block by UCL1684 [rSK2(Y246L) IC_{50}, 560 ± 84 pM, $n = 6$, $P = 0.1882$; rSK2(S245T) IC_{50}, 376 ± 101 pM, $n = 6$, $P = 0.7540$] (Fig. 4*D* and Table 1). These data show that UCL1684 does not directly bind to the S3–S4 loop, but that the influence of the S3–S4 loop on the pore structure affects UCL1684 sensitivity.

Heteromeric Channels Suggest That the S3–S4 Loop Overlaps the Outer Pore of the Adjacent Subunit. Our data are consistent with the structural modeling that placed apamin interacting with the outer pore of the SK channel (7). This model suggested that arginine 13 of the toxin was orientated away from the channel pore to interact with the S3–S4 extracellular loop (7). This proposed binding places apamin distant from the inner pore and ion conduction pathway, suggesting that it blocks by using an allosteric mechanism. These data are consistent with the finding that apamin binds to both SK2 and SK3 with the same high affinity ($K_D \sim$ 5 pM for both subtypes) (7) but requires significantly higher concentrations to block functional current (IC_{50} values of ~100 pM and 630 pM, respectively). A Hill coefficient of greater than unity was observed in this study and previous studies of apamin block of wild-type rSK2 and hSK3, suggesting positive cooperativity of apamin block (7). Coexpression of apamin-sensitive rSK2 subunits with an apamin-insensitive mutant [rSK2(H337N)] produces heteromeric channels with two sensitivities to apamin, where the efficacy of apamin is influenced positively by interactions between adjacent subunits (7). Coexpression of apamin-sensitive rSK2 and apamin-insensitive rSK1* subunits is predicted to form a mix of homomeric channels from each subunit and heteromeric channels. The probabilities of the occurrence of different predicted stoichiometries of channel subunit assembly follow a binomial distribution if it is assumed that the probability of the inclusion of each subunit into the channel tetramer is equivalent, with 60% of the current originating from channels that contain at least two adjacent rSK2 subunits (7). Expressed heteromeric channel current is predicted to be blocked by apamin, with a concentration-inhibition curve best fit by the sum of two Hill equations, where the high-sensitivity component corresponds to block of channels containing at least two adjacent rSK2 subunits and the low-sensitivity component arises from block of tetrameric channels not containing adjacent rSK2 subunits (7). This low-sensitivity component can include block by only one apamin molecule (7). Block by apamin of current from coexpressed rSK2 and SK1* subunits loosely follows the expected binomial distribution of channels, with current block displaying a high-sensitivity component (comprising 67.2 ± 4.7% of sensitive current, $n = 6$) displaying an IC_{50} ($IC_{50,a}$) of 450 ± 95 pM and a low-sensitivity component displaying an IC_{50} ($IC_{50,b}$) of 8.41 ± 3.38 nM ($n = 6$) (Fig. 5*A* and Table 2). Coexpression of rSK2 with rSK2(YA246/7LV) results in a distribution of heteromeric channels with a very different pharmacological profile to block by apamin compared with heteromeric rSK2-rSK1* channel current. The high-sensitivity component of block of the rSK2-rSK2

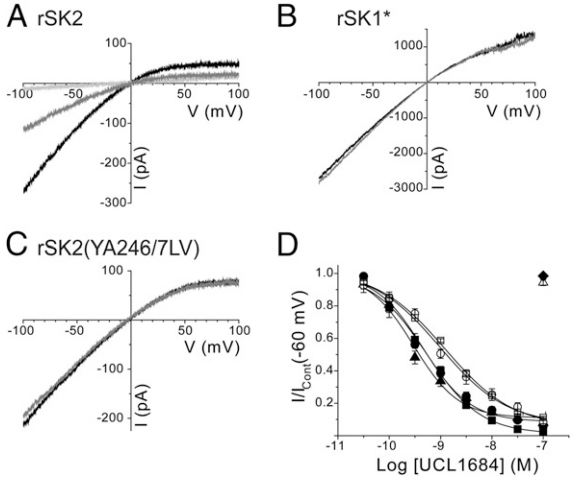

Fig. 4. UCL1684 does not directly interact with the S3–S4 extracellular loop of SK channels. (*A*–*C*) Currents derived by voltage ramps from −100 to +100 mV evoked by expressed rSK2 (*A*), rSK1* (*B*), and rSK2(YA246/7LV) (*C*) subunits. Application of 1 nM UCL1684 (gray trace) inhibited ~65% of rSK2 current, whereas addition of 100 nM UCL1684 (light gray) inhibited ~95% of current. In contrast, rSK1* and rSK2(YA246/7LV) were UCL1684 insensitive. (*D*) Concentration-inhibition relationships for UCL1684 inhibition of expressed rSK2 (●), rSK2(Y246L) (■), rSK2(S245T) (▲), hSK1 (○), rSK1(LV213/4YA) (□), rSK1* (△), and rSK2(YA246/7LV) (◆) current.

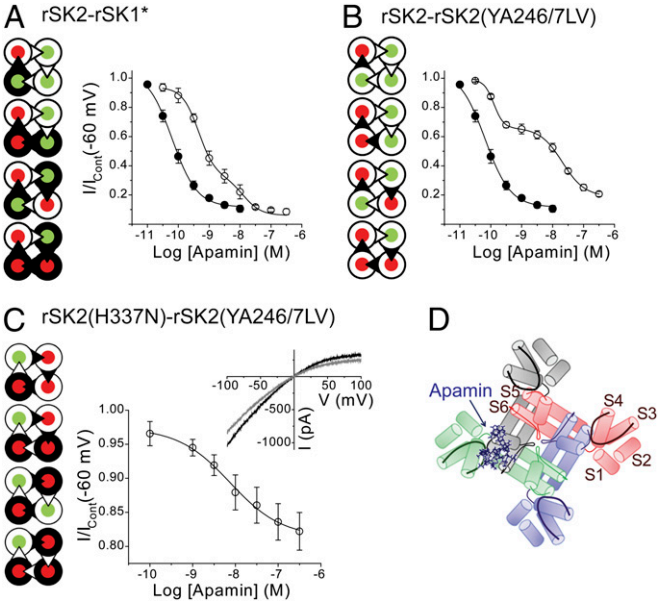

Fig. 5. Apamin-sensitive current produced by expression of two apamin-insensitive subunits. (*A*, *Left*) Hypothetical arrangement of apamin binding sites within rSK2-rSK1* heteromeric channels. The rSK2 subunits are pictured as ◇, and rSK1* subunits are shown as ◆. The S3–S4 extracellular loop is depicted as the triangle, with a loop containing the SYA motif (e.g., rSK2) colored white and a loop containing the SLV motif (e.g., rSK1*) colored black. Overlapping the S3–S4 extracellullar loop of rSK1* with the outer pore region of an adjacent rSK2 subunit produces a combined subunit that is unable to bind apamin (◇▷). In contrast, the overlap of the S3–S4 extracellular loop of rSK2 with the outer pore of an adjacent rSK1* subunit produces a combined subunit that binds apamin (▽◆). (*Right*) Comparison of sensitivity to apamin of homomeric wild-type rSK2 (●) and current produced by coexpression of rSK2 and rSK1* subunits (○). Heteromeric rSK2-rSK1* channel current displays block by apamin with two affinities. (*B*, *Left*) Arrangement of rSK2 subunits (◇) and rSK2(YA246/7LV) subunits (◇) to produce a subunit that is unable to bind apamin (◇▷ or ◆▷). The higher sensitivity of the high-sensitivity component of rSK2-rSK2(YA246/7LV) current to apamin and greater cooperativity of binding can be attributed to the overlap of the S3–S4 loop from rSK2 with the adjacent rSK2(YA246/7LV) subunit outer pore. (*Right*) Coexpressed rSK2-rSK2(YA246/7LV) subunits produce current that is blocked by apamin with two sensitivities (○), compared with wild-type rSK2 (●). Apamin block displays a higher-sensitivity component than that seen with block of rSK2-rSK1* heteromeric current. (*C*, *Left*) Coexpression of apamin-insensitive outer pore mutant rSK2(H337N) subunits (◆) with apamin-insensitive S3–S4 loop mutant rSK2(YA246/7LV) subunits (◇) produces a combined subunit that can bind apamin (◆◁). (*Right*) Coexpressed rSK2(H337N)-rSK2(YA246/7LV) subunits produce apamin-sensitive current (○). (*Inset*) Outside-out macropatch currents derived by voltage ramps from −100 to +100 mV imposed on cells coexpressing rSK2(H337N) and rSK2(YA246/7LV) and block by 100 nM apamin (gray trace). (*D*) Prediction of the location of the S3–S4 loop in the SK tetramer.

(YA246/7LV) heteromeric channel current by apamin is significantly more potent than that seen with rSK2-rSK1* ($IC_{50,a}$, 117 ± 14 pM, $n = 6$, $P = 0.0081$) (Fig. 5*B* and Table 2). In contrast, the low-sensitivity component displays a significantly larger IC_{50} than that seen for block of rSK2-rSK1* current ($IC_{50,b}$, 19.9 ± 2.51 nM, $n = 6$, $P = 0.0208$) (Table 2). It should be noted that block of current from coexpression of rSK2-rSK2(YA246/7LV) subunits did not follow the expected binomial distribution of assembled channels, with only 44.2 ± 5.1% of current being blocked with high sensitivity. These data suggest that either the expression of each subunit is not equal or the probability of any subunit being included in the channel tetramer is not equivalent.

Our and previous data have shown that apamin interacts with both the S3–S4 extracellular loop and the outer pore of SK channels to cause block (7). The finding that a component of block by apamin of rSK2-rSK2(YA246/7LV) heteromeric channel current is of higher sensitivity than is seen with rSK2-rSK1* channel current requires interpretation. Both homomeric rSK2 (YA246/7LV) and rSK1* channel currents are insensitive to block by apamin, as they both share the same SLV amino acid motif in the S3–S4 extracellular loop. However, although they share very similar pore shapes (as seen by sensitivity to dTC and TEA), they do possess different pore sequences (Fig. 1) (9). The outer pore region of rSK1 contains crucial differences in its sequence known to greatly reduce sensitivity to apamin (Fig. 1), whereas rSK2(YA246/7LV) contains an outer pore sequence identical to the highly apamin-sensitive rSK2 wild-type (Fig. 1) (13). It is possible that the increased sensitivity of the high-affinity component of block of rSK2-rSK2(YA246/7LV) heteromeric channel current arises because the S3–S4 loop region of one subunit overlaps with the outer pore region of the adjacent subunit, compared with coexpressed rSK2-rSK1* heteromeric current. Proposed tetrameric channel assemblies are shown in Fig. 5 *A* and *B*, where the illustrated stoichiometries of channel subunit assembly follow a binomial distribution but the overlap of the S3–S4 loop region determines which subunit combination permits binding of apamin. This proposed arrangement offers an explanation of the difference in sensitivity of the high-affinity component of block seen between the different coexpressed heteromers. This proposal is because apamin sensitivity of these two heteromers would be identical if the S3–S4 loop overlaps the outer pore of the same subunit. However, if the S3–S4 loop of one subunit overlaps the adjacent subunit, distinct apamin binding sites would be revealed (Fig. 5 *A* and *B*). Coexpression of two apamin-insensitive subunits, one being the apamin-insensitive S3–S4 loop mutant rSK2(YA246/7LV) and the other being the outer pore mutant rSK2(H337N) (7), will test this hypothesis. If the S3–S4 loop of each subunit interacts with its own outer pore region, then none of the current should be sensitive to apamin. However, if the loop of one subunit overlaps the adjacent subunit, then a population of heteromeric channels would be formed that would have the loop from rSK2(H337N) (which will bind apamin) and the outer pore of rSK2(YA246/7LV) (whose pore sequence will support block). This population would be sensitive to apamin (Fig. 5*C*). Coexpression of the two apamin-insensitive subunits produces a resultant current that is apamin sensitive, with 17 ± 3% of the current blocked by the toxin. The IC_{50} of 5.65 ± 1.34 nM ($n = 6$) (Fig. 5*C*) is comparable with the low-sensitivity component of the rSK2-rSK1* and rSK2-rSK2 (YA246/7LV) heteromers. The Hill coefficient was 1.1 ± 0.2, indicating no cooperativity of apamin binding, as predicted by the overlapping loop model where no adjacent apamin-sensitive binding sites are present. Finally, a lower percentage of the current is blocked than would be predicted by binomial theory (~85%). As both these mutations have been shown to result in a significant change in pore shape, these results could suggest that these mutant subunits preferentially express as homomeric, apamin-insensitive channels.

Discussion

The S3–S4 extracellular loop is crucial in dictating the sensitivity of SK channels to block by apamin. The three-amino-acid motif in the S3–S4 loop of SK channels (SLV in rSK1, TYA in hSK1, SYA in SK2, and SYT in SK3) is an essential molecular determinant for apamin sensitivity. These data resolve the dichotomy that rSK1 is insensitive to apamin (11, 12), yet has the same pore sequence as the apamin-sensitive hSK1. It is because rSK1 displays SLV in the S3–S4 loop that prevents binding of apamin. Essentially, this finding and the observation of apamin-sensitive channels being formed from the coexpression of the two apamin-insensitive subunits indicate that apamin must bind to the S3–S4 extracellular loop to block. Structural modeling and mutagenesis have indicated that apamin binds to the outer pore (7), presumably a binding site that overlaps with that used by UCL1684. Apamin must bind to both the S3–S4 extracellular loop and the outer pore to block SK channel current by an allosteric mechanism. In contrast, UCL1684 does not interact with the S3–S4 loop and presumably blocks SK channel current by binding to the channel outer pore using an allosteric mechanism. This difference is probably why UCL1684 shows poor selectivity in blocking SK channel subtypes compared with apamin (9).

The affinity for apamin binding is higher than the sensitivity of functional block (7). This separation of binding and block affinities can be considered as a measure of the toxin's efficacy to block SK channel current (9). This efficacy was determined by comparison of the binding affinity of ^{125}I-apamin and block of functional current by the native toxin (7, 9). Binding of ^{125}I-apamin to rSK2 yields a K_D of ~5 pM, whereas competition of ^{125}I-apamin binding by native apamin yields a K_i of 2.7 ± 0.8 pM ($n = 7$) (18). These data indicate that efficacy has been slightly underestimated in previous studies.

Functional block by apamin displays positive cooperativity, despite a lack of cooperativity of ^{125}I-apamin binding (7). We have previously shown in coexpression studies of rSK2 with an apamin-insensitive mutant that the efficacy of apamin is influenced positively by interactions between subunits (7). This result was also observed for heteromeric channel current formed from assembly of coexpressed rSK2 and rSK1* or rSK2(YA246/7LV) subunits, as the Hill coefficients for the high-sensitivity component of apamin block were greater than unity (Table 2). In contrast, the low-sensitivity components of block by apamin of either heteromeric rSK2-rSK1* or rSK2-rSK2(YA246/7LV) channels displayed a Hill coefficient of close to unity, as did current formed by coexpression of rSK2(H337N)-rSK2(YA246/7LV). These data support the proposal that high sensitivity to block by apamin occurs by cooperativity between adjacent subunits. It is likely that the simultaneous binding of apamin to both the S3–S4 extracellular loop and the outer pore of an adjacent subunit causes block to exhibit positive cooperativity. In contract, block by UCL1684 results only from binding to the channel outer pore and this block does not exhibit cooperativity (Tables 1 and 2).

Current carried by SK channels exhibits significant inward rectification in both physiological and symmetrical potassium concentrations (7, 14, 19), which is likely the result of a combination of block by intracellular divalent cations (20) and the presence of three charged residues near the inner mouth of the pore (19). Rectification can be quantified by dividing the current measured at +60 mV by that observed at −60 mV to give a rectification index (RI). We observed that current carried by both rSK1* and rSK2(YA246/7LV) displayed less inward rectification at depolarized levels than seen with wild-type rSK2, with RI values ranging from 0.61 ± 0.06 ($n = 9$) and 0.58 ± 0.03 ($n = 19$) for rSK1* and rSK2(YA246/7LV), respectively, to 0.40 ± 0.02 ($n = 23$) for wild-type rSK2 and 0.35 ± 0.03 ($n = 7$) for the heteromeric rSK2-rSK1* current. Our data shows that rSK1* and rSK2(YA246/7LV) have outer and inner pore shapes that are similar to each other, but are different from wild-type rSK2. These different pore shapes are extrapolated from the sensitivities of current to block by either dTC (outer pore) or TEA (inner pore). TEA is proposed to block SK current by interacting

with the channel pore close to the selectivity filter (7), within three amino acid residues of serine 359 that is proposed to confer rectification by binding a divalent ion (20). Therefore, it is likely that the observed differences in rectification between wild-type SK channels and loop mutants result from different inner pore shapes imposed by interaction with the outer pore and the S3–S4 loop. It is possible that these different inner pore shapes affect the affinity of divalent cations to bind to serine 359, resulting in a reduction of rectification for both rSK1 and rSK2(YA246/7LV).

Our results strongly suggest that the binding pocket for apamin is produced by two adjacent subunits, with the S3–S4 loop interacting directly with the outer pore of the adjacent subunit. Our data suggest that the channel subunits might be arranged as shown in Fig. 5*D*. This is of particular relevance when it is considered that subtypes of SK channels show overlapping expression patterns in the nervous system and periphery. It is known that each SK channel subtype can form heteromeric channels with each other subtype (5, 21), and it is the presence of heteromeric SK channels that introduces a new level of complication to the development of treatments targeting SK channels. Previous studies have focused on the development of subtype-specific blockers, assuming the native population of SK channels would be primarily homomeric. The high level of colocalization of SK channels throughout the body, combined with the ability of SK channels to form heteromers, suggests that a blocker targeting one SK subtype may not be therapeutically useful. Indeed, the majority of the SK current recorded in the SK2-rSK1* coexpression studies was found to consist of heteromeric channels, with indistinguishable levels of homomeric channels. In native cells, coimmunoprecipitation of SK1, SK2, and SK3 in human and mouse atrial myocytes indicated that all three subtypes were present as heteromeric complexes (22). Similarly, a concentration response curve of block of the current proposed to underlie the medium afterhyperpolarization in rat CA1 hippocampal neurons by apamin deduced an IC_{50} of ~480 pM, approximately sevenfold less sensitive than homomeric SK2 and comparable with the high-sensitivity component of the rSK2-rSK1* heteromer (450 ± 95 pM), suggesting a predominantly heteromeric population of SK channels (23). Although our data using rSK1* cannot definitively prove that these subunits can form heteromeric channels, it is reported that heterologous coexpression of wild-type rSK1 and rSK2 in HEK293 cells produces functional heteromeric channels (5). It is clear that should SK channel subunits coassemble into heteromeric channels in native cells, a wide range of unique binding sites are likely to be created at the S3–S4 loop–outer pore region. The small differences in the SK2 and SK3 S3–S4 loop regions, and the SK1 outer pore region, may provide the means to develop heteromeric-specific SK channel blockers. A blocker specific for a heteromeric channel could be used to specifically target a region known to express multiple subunits, resulting in a lower side-effect profile.

Experimental Procedures

Transient Expression in HEK293 and tsA201 Cells. Wild-type rat SK2 (GenBank accession no. U69882.1) and human SK1 (GenBank accession no. NM002248.3) channel DNAs were subcloned into the mammalian plasmid expression vectors pcDNA3 (Invitrogen). A chimeric channel consisting of residues 1 to 372 of rSK1 (GenBank accession no. NM019313.1) and 406 to 580 of rSK2 was generated as described previously and subcloned into pFLAG-CMV2 (11); this construct is termed rSK1* in this study. Single and double point mutations were introduced using the QuikChange XL site-directed mutagenesis kit (Stratagene-Agilent) and subsequently confirmed by dye termination DNA sequencing.

HEK293 and tsA201 cell lines were maintained as described previously (7). Cells were transiently transfected using polyethyleneimine (Alfa Aesar) by combining channel plasmid DNA with enhanced green fluorescent protein DNA in a ratio of 1:5 (maximal plasmid content: 1.5 μg). The ratio of coexpressed subunit plasmid DNA was 1:1. Cells expressing enhanced green fluorescent protein were used for electrophysiology 16 to 24 h after transfection.

Expressed SK currents were recorded in the outside-out patch configuration, with the concentration-dependence of block by apamin (Sigma-Alrich), UCL1684 (Tocris Biosciences), dTC (Sigma-Aldrich), and TEA (Sigma-Aldrich) being determined by rapid solution exchange (*SI Experimental Procedures*) (7). Binding of ^{125}I-apamin has been described previously (7) and is presented in *SI Experimental Procedures*.

All numerical values are expressed as mean ± SEM. Statistical analysis was performed using GraphPad Prism 4.0 (GraphPad Software). Data were analyzed with a Student's *t* test or one-way ANOVA. Representative current traces were drawn using Origin 6.0 (Microcal Software).

ACKNOWLEDGMENTS. We thank Christelle Gillissen for technical support in binding experiments and Prof. David Jane for critical reading of the manuscript. J.-F.L. is Research Director of the Belgian National Fund for Scientific Research. This work was supported by Grant IAP P6/31 from the Belgian Science Policy.

1. Sailer CA, et al. (2002) Regional differences in distribution and functional expression of small-conductance Ca^{2+}-activated K^+ channels in rat brain. *J Neurosci* 22: 9698–9707.
2. Sailer CA, Kaufmann WA, Marksteiner J, Knaus HG (2004) Comparative immunohistochemical distribution of three small-conductance Ca^{2+}-activated potassium channel subunits, SK1, SK2, and SK3 in mouse brain. *Mol Cell Neurosci* 26:458–469.
3. Stocker M, Pedarzani P (2000) Differential distribution of three $Ca^{(2+)}$-activated $K^{(+)}$ channel subunits, SK1, SK2, and SK3, in the adult rat central nervous system. *Mol Cell Neurosci* 15:476–493.
4. van der Staay FJ, Fanelli RJ, Blokland A, Schmidt BH (1999) Behavioral effects of apamin, a selective inhibitor of the $SK_{(Ca)}$-channel, in mice and rats. *Neurosci Biobehav Rev* 23:1087–1110.
5. Benton DC, et al. (2003) Small conductance Ca^{2+}-activated K^+ channels formed by the expression of rat SK1 and SK2 genes in HEK 293 cells. *J Physiol* 553(Pt 1):13–19.
6. Köhler M, et al. (1996) Small-conductance, calcium-activated potassium channels from mammalian brain. *Science* 273:1709–1714.
7. Lamy C, et al. (2010) Allosteric block of $K_{Ca}2$ channels by apamin. *J Biol Chem* 285: 27067–27077.
8. Nolting A, Ferraro T, D'hoedt D, Stocker M (2007) An amino acid outside the pore region influences apamin sensitivity in small conductance Ca^{2+}-activated K^+ channels. *J Biol Chem* 282:3478–3486.
9. Weatherall KL, Goodchild SJ, Jane DE, Marrion NV (2010) Small conductance calcium-activated potassium channels: From structure to function. *Prog Neurobiol* 91:242–255.
10. Grunnet M, et al. (2001) Pharmacological modulation of SK3 channels. *Neuropharmacology* 40:879–887.
11. D'hoedt D, Hirzel K, Pedarzani P, Stocker M (2004) Domain analysis of the calcium-activated potassium channel SK1 from rat brain. Functional expression and toxin sensitivity. *J Biol Chem* 279:12088–12092.
12. Corrêa SA, Müller J, Collingridge GL, Marrion NV (2009) Rapid endocytosis provides restricted somatic expression of a K^+ channel in central neurons. *J Cell Sci* 122: 4186–4194.
13. Ishii TM, Maylie J, Adelman JP (1997) Determinants of apamin and d-tubocurarine block in SK potassium channels. *J Biol Chem* 272:23195–23200.
14. Goodchild SJ, Lamy C, Seutin V, Marrion NV (2009) Inhibition of $K_{(Ca)}2.2$ and $K_{(Ca)}2.3$ channel currents by protonation of outer pore histidine residues. *J Gen Physiol* 134: 295–308.
15. Bowden SE, Fletcher S, Loane DJ, Marrion NV (2001) Somatic colocalization of rat SK1 and D class (Ca(v)1.3) L-type calcium channels in rat CA1 hippocampal pyramidal neurons. *J Neurosci*, 21(20): RC175, 1–6.
16. Campos Rosa J, et al. (2000) Synthesis, molecular modeling, and pharmacological testing of bis-quinolinium cyclophanes: Potent, non-peptidic blockers of the apamin-sensitive $Ca^{(2+)}$-activated $K^{(+)}$ channel. *J Med Chem* 43:420–431.
17. Dunn PM (1999) UCL 1684: A potent blocker of Ca^{2+}-activated K^+ channels in rat adrenal chromaffin cells in culture. *Eur J Pharmacol* 368(1):119–123.
18. Finlayson K, et al. (2001) Characterisation of [(^{125})I]-apamin binding sites in rat brain membranes with HE293 cells transfected with SK channel subtypes. *Neuropharmacology* 41:341–350.
19. Li W, Aldrich RW (2011) Electrostatic influences of charged inner pore residues on the conductance and gating of small conductance Ca^{2+} activated K^+ channels. *Proc Natl Acad Sci USA* 108:5946–5953.
20. Soh H, Park CS (2002) Localization of divalent cation-binding site in the pore of a small conductance $Ca^{(2+)}$-activated $K^{(+)}$ channel and its role in determining current-voltage relationship. *Biophys J* 83:2528–2538.
21. Monaghan AS, et al. (2004) The SK3 subunit of small conductance Ca^{2+}-activated K^+ channels interacts with both SK1 and SK2 subunits in a heterologous expression system. *J Biol Chem* 279:1003–1009.
22. Tuteja D, et al. (2010) Cardiac small conductance Ca^{2+}-activated K^+ channel subunits form heteromultimers via the coiled-coil domains in the C termini of the channels. *Circ Res* 107:851–859.
23. Stocker M, Krause M, Pedarzani P (1999) An apamin-sensitive Ca^{2+}-activated K^+ current in hippocampal pyramidal neurons. *Proc Natl Acad Sci USA* 96:4662–4667.